

(b) The most probable distance of a $2s$ electron from the nucleus may be determined by plotting the radial distribution function against r/a_0 and using the trace function of the plotting software to evaluate the coordinates of the maximum. The following function is plotted in Figure 9.3. The plot reveals that $r_{\max} = 5.235 a_0$.

$$P_{2s} = 4\pi r^2 \psi_{2s}^2 [13.7a] = 4\pi r^2 \left\{ \left(\frac{1}{32\pi a_0^3} \right)^{1/2} \left(2 - \frac{r}{a_0} \right) e^{-r/2a_0} \right\}^2$$

$$= \frac{1}{8a_0^3} \left(2 - \frac{r}{a_0} \right)^2 r^2 e^{-r/a_0} = \boxed{\frac{1}{8a_0} (2-x)^2 x^2 e^{-x} \text{ where } x = r/a_0}$$

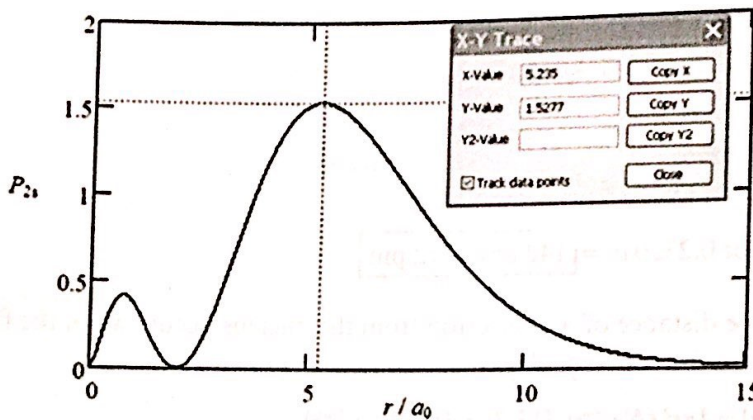


Figure 9.3

(c) Let $x = r/a_0$, then

$$P_{2s} = \frac{1}{8a_0} \{x^2(2-x)^2 e^{-x}\} = \frac{1}{8a_0} (4x^2 - 4x^3 + x^4) e^{-x}$$

$$\frac{dP_{2s}}{dr} = \frac{dx}{dr} \frac{dP_{2s}}{dx} = \frac{1}{8a_0^2} \frac{d\{(4x^2 - 4x^3 + x^4)e^{-x}\}}{dx}$$

$$= \frac{1}{8a_0^2} \{(8x - 12x^2 + 4x^3)e^{-x} + (4x^2 - 4x^3 + x^4)(-e^{-x})\} = \frac{1}{8a_0^2} \{8 - 16x + 8x^2 - x^3\} xe^{-x}$$

$$= -\frac{1}{8a_0^2} \times (x-2) \times (x^2 - 6x + 4) xe^{-x}$$

The derivative equals zero when $x = r/a_0 = 0, 3 - 5^{1/2}, 2, 3 + 5^{1/2}$, and ∞ . These correspond to the radial distribution function being a minimum, a maximum, a minimum, a maximum, and a minimum, respectively. The following ratio identifies the maximum that is most probable.

$$\frac{P_{2s}(x = 3 + 5^{1/2})}{P_{2s}(x = 3 - 5^{1/2})} = \frac{[(4x^2 - 4x^3 + x^4)e^{-x}]_{x=3+5^{1/2}}}{[(4x^2 - 4x^3 + x^4)e^{-x}]_{x=3-5^{1/2}}} = \frac{1.528}{0.415} = 3.68$$

The most probable distance is $\boxed{(3 + 5^{1/2})a_0}$.

E9.39

There are two methods that can be used to locate the radial nodes of a hydrogen atom orbital. We could find a textbook plot of the radial function $R_{n,l}$ against r/a_0 and read the node values directly from the plot. Alternatively, we could search an advanced textbook on physical chemistry to find the mathematical form for $R_{n,l}$ and analyze the function for its nodes.

(a) Figure 9.4 is a typical plot for the $3s$ hydrogen orbital. The nodes occur when the radial function passes through zero. These occur when $r = \boxed{1.9 a_0 \text{ and } 7.1 a_0}$

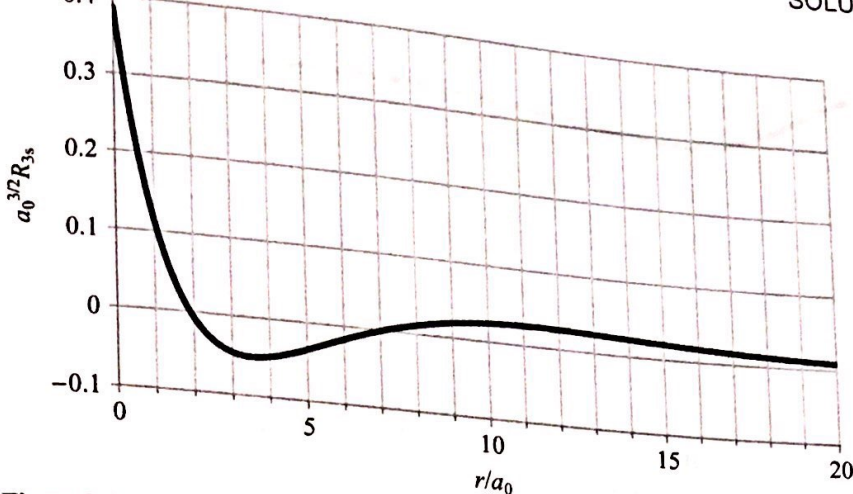


Figure 9.4

(b) Finding the nodes of the 4s orbital of a hydrogen atom is a greater challenge. Few textbooks display a plot of this radial wavefunction so it becomes necessary to find the mathematical form of this function. Eqn 10.14 of P. Atkins and J. de Paula, *Physical Chemistry*, 8th edn, Freeman, 2006 reports that the radial function is

$$R_{n,l} = N_{n,l} \rho^l L_{n+l}^{2l+1}(\rho) e^{-\rho/2} \quad \text{where} \quad \rho = \frac{2r}{na_0}$$

$L_{n+l}^{2l+1}(\rho)$ is the associated Laguerre polynomial and examination of the above radial function indicates that the radial nodes occur when $L_{n+l}^{2l+1}(\rho)$ equals zero. Thus, we must solve for the zeros of the associated Laguerre polynomial for the 4s orbital. L. Pauling and E. Wilson Jr., *Introduction to Quantum Mechanics with Applications to Chemistry*, McGraw-Hill, New York (1935) report the following form for the associated Laguerre polynomial.

$$\frac{L_{n+l}^{2l+1}(\rho)}{\{(n+l)!\}^2} = \sum_{k=0}^{n-l-1} \frac{(-1)^{k+1} \rho^k}{(n-l-1-k)!(2l+1+k)!k!} \quad \text{where } 0! = 1 \text{ and } m! = m \times (m-1) \times (m-2) \times \dots \times 1$$

For the 4s orbital we use $n = 4$, $l = 0$, and $\rho = \frac{r}{2a_0}$.

$$\begin{aligned} \frac{L_4^1(\rho)}{\{4!\}^2} &= \sum_{k=0}^3 \frac{(-1)^{k+1} \rho^k}{(3-k)!(1+k)!k!} \\ &= \frac{(-1)^1 \rho^0}{(3)!(1)!0!} + \frac{(-1)^2 \rho^1}{(2)!(2)!1!} + \frac{(-1)^3 \rho^2}{(1)!(3)!2!} + \frac{(-1)^4 \rho^3}{(0)!(4)!3!} \\ &= -\frac{1}{6} + \frac{\rho}{4} - \frac{\rho^2}{12} + \frac{\rho^3}{144} = \frac{1}{144}(\rho^3 - 12\rho^2 + 36\rho - 24) \end{aligned}$$

Thus, the nodes of the 4s orbital occur when

$$\rho^3 - 12\rho^2 + 36\rho - 24 = 0$$

The roots of this polynomial can be found with either the root function or the numeric solver of the modern scientific calculator. The roots found are $\rho = 0.936$, 3.305 , and 7.759 . Since $r = 2a_0\rho$, the nodes are at

$$r = \boxed{1.87 a_0, 6.61 a_0, \text{ and } 15.5 a_0}$$

The plot of R_{4s} against r/a_0 , shown in Figure 9.5, confirms this result.

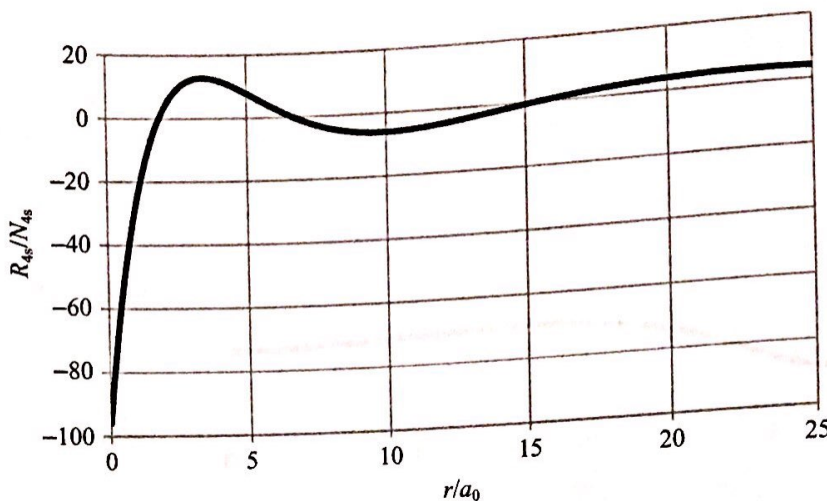


Figure 9.5

- E9.40** Look for values of θ for which $\sin \theta$ or $\cos \theta$ go to zero. $\sin \theta$ goes to zero at $\theta = [0^\circ \text{ and } 180^\circ]$; $\cos \theta$ at $[90^\circ \text{ and } 270^\circ]$.

- E9.41** Identify l and use angular momentum $= \{l(l+1)\}^{1/2} \hbar$

(a) $l=0$, so $\boxed{\text{ang. mom.} = 0}$

(b) $l=0$, so $\boxed{\text{ang. mom.} = 0}$

(c) $l=2$, so $\boxed{\text{ang. mom.} = \sqrt{6} \hbar}$

(d) $l=1$, so $\boxed{\text{ang. mom.} = \sqrt{2} \hbar}$

(e) $l=1$, so $\boxed{\text{ang. mom.} = \sqrt{2} \hbar}$

The total number of nodes is equal to $n - 1$, and the number of angular nodes is equal to l ; hence the number of radial nodes is equal to $n - 1 - l$. We can draw up the following table:

	1s	3s	3d	2p	3p
n, l	1,0	3,0	3,2	2,1	3,1
Ang. nodes	0	0	2	1	1
Rad. nodes	0	2	0	0	1

- E9.42** For a given l there are $2l + 1$ values of m_l and hence $2l + 1$ orbitals. Each orbital may be occupied by two electrons. Therefore, the maximum occupancy is $2(2l + 1)$.

	l	$2(2l + 1)$
(a)	0	2
(b)	3	14
(c)	5	22

E9.43

(a) Periodic table

1s	H	He		B	C	N	O	F	Ne	Na	Mg	2p
2s	Li	Be		P	S	Cl	Ar	K	Ca	Sc	Ti	3p
3s	Al	Si										
4s	V	Cr										

(c) Probably N because it has 5 electrons in its valence shell which corresponds to half-filled, like carbon.

(b) "Noble gases"

E9.44

The electron configurations of the ions are:



$\boxed{\text{Fe}^{2+}}$ is expected to be larger. The reason is the repulsion between electrons in the same outer sub-shell. The more electrons, the greater the overall repulsions, leading to a greater average distance from the nucleus for the outer electrons and hence increased ionic size.

E9.45

See Figure 9.6 for the ionization trends of Group 13.

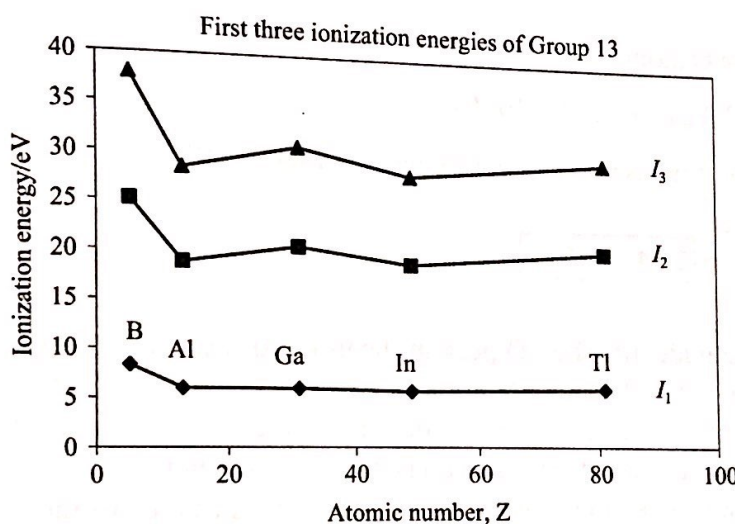
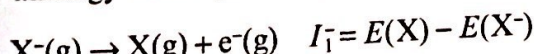


Figure 9.6

Trends:

- (i) $I_1 < I_2 < I_3$ because of decreased nuclear shielding as each successive electron is removed.
- (ii) The ionization energies of boron are much larger than those of the remaining group elements because the valence shell of boron is very small and compact with little nuclear shielding. The boron atom is much smaller than the aluminum atom.
- (iii) The ionization energies of Al, Ga, In, and Tl are comparable, even though successive valence shells are further from the nucleus because the ionization energy decrease expected from large atomic radii is balanced by an increase in effective nuclear charge.

E9.46

By analogy with equation [9.37] the ionization energy of an anion, I_1^- , is for the reaction

while the electron affinity of equation [9.38] is for the reaction

10 The chemical bond

Answers to discussion questions

D10.1

Our comparison of the two theories will focus on the manner of construction of the trial wavefunctions for the hydrogen molecule in the simplest versions of both theories. In the valence-bond method, the trial function is a linear combination of two simple product wavefunctions, in which one electron resides totally in an atomic orbital (AO) on atom A, and the other totally in an orbital on atom B. See text Figure 10.2. There is no contribution to the wavefunction from products in which both electrons reside on either atom A or B.

$$\psi_{H-H}(1, 2) = \psi_A(1)\psi_B(2) + \psi_A(2)\psi_B(1) \quad [10.1]$$

So the valence-bond approach undervalues, by totally neglecting, any ionic contribution to the trial function. It is a totally covalent function.

The modern one-electron molecular orbital (MO) extends throughout the molecule and is written as a linear combination of atomic orbitals (LCAO).

$$\psi_{MO}(1) = c_A\psi_A(1) + c_B\psi_B(1) \quad [10.4a]$$

The squares of the coefficients give the relative proportions of the AO contributing to the MO.

The two-electron molecular orbital function for the hydrogen molecule is a product of two one-electron MOs. That is

$$\begin{aligned}\psi &= [c_A\psi_A(1) + c_B\psi_B(1)] \times [c_A\psi_A(2) + c_B\psi_B(2)] \\ &= c_A^2\psi_A(1)\psi_A(2) + c_B^2\psi_B(1)\psi_B(2) + c_Ac_B\psi_A(1)\psi_B(2) + c_Ac_B\psi_A(2)\psi_B(1)\end{aligned}$$

The first two terms are ionic forms for which both electrons are on either atom A or on atom B. The molecular orbital approach greatly overvalues the ionic contributions. At these crude levels of approximation, the valence-bond method gives dissociation energies closer to the experimental values. However, more sophisticated versions of the molecular orbital approach are the method of choice for obtaining quantitative results on both diatomic and polyatomic molecules.

D10.2

Consider the case of the carbon atom. Mentally we break the process of hybridization into two major steps. The first is promotion, in which we imagine that one of the electrons in the 2s orbital of carbon ($2s^22p^2$) is promoted to the empty 2p orbital giving the configuration $2s2p^3$. In the second step we mathematically mix the four orbitals by way of the specific linear combinations in eqns 10.2a corresponding to the sp^3 hybrid orbitals. There is a principle of conservation of orbitals that enters here. If we mix four unhybridized atomic orbitals we must end up with four hybrid orbitals. In the construction of the sp^2 hybrids we start with the 2s orbital and two of the 2p orbitals, and after mixing we end up with three sp^2 hybrid orbitals. In the sp case we start with the 2s orbital and one of the 2p orbitals. Equations 10.2b and 10.2c present the LCAO for the sp^2 and sp hybrid orbitals; text Figures 10.7 and 10.9 describe the orientations of sp^3 and sp^2 hybrid orbitals. The justification for

all of this is in a sense the First Law of Thermodynamics. Energy is a state function and therefore its value is determined only by the final state of the system, not by the path taken to achieve that state, and the path can even be imaginary.

- D10.3** Both the Pauling and Mulliken methods for measuring the attracting power of atoms for electrons seem to make good chemical sense.

Pauling electronegativity scale:

$$|\chi_A - \chi_B| = 0.102 \times (\Delta E / \text{kJ mol}^{-1})^{1/2} \quad [10.8a], \text{ where } \Delta E = E(A-B) - \frac{1}{2}\{E(A-A) + E(B-B)\}$$

Mulliken electronegativity scale:

$$\chi = \frac{1}{2}(I + E_{ea}) \quad [10.8c]$$

If we look at the Pauling scale, we see that if $E(A-B)$ were equal to $\frac{1}{2}[E(A-A) + E(B-B)]$ the calculated electronegativity difference would be zero, as expected for completely non-polar bonds. Hence, any increased strength of the A—B bond over the average of the A—A and B—B bonds, can reasonably be thought of as being due to the polarity of the A—B bond, which in turn is due to the difference in electronegativity of the atoms involved. Therefore, this difference in bond strengths can be used as a measure of electronegativity difference. To obtain numerical values for individual atoms, a reference state (atom) for electronegativity must be established. The value for fluorine is arbitrarily set at 4.0.

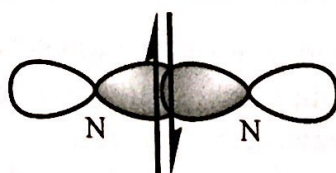
The Mulliken scale may be more intuitive than the Pauling scale because we are used to thinking of ionization energies and electron affinities as measures of the electron attracting powers of atoms. The choice of factor $\frac{1}{2}$, however, is arbitrary, though reasonable, and no more arbitrary than the specific form that defines the Pauling scale.

- D10.4** The ground electronic configurations of the valence electrons are found in text Figures 10.30, 10.31, 10.35.

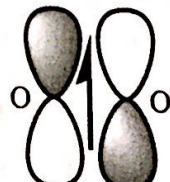
N_2	$1\sigma_g^2 1\sigma_u^2 1\pi_g^4 2\sigma_g^2$	$b = 3$	$2S + 1 = 1$
O_2	$1\sigma_g^2 1\sigma_u^2 2\sigma_g^2 1\pi_u^4 1\pi_g^2$	$b = 2$	$2S + 1 = 3$
NO	$1\sigma^2 2\sigma^2 3\sigma^2 1\pi^4 2\pi^1$	$b = 2\frac{1}{2}$	$2S + 1 = 2$

The following figures show HOMOs of each. Shaded versus unshaded AO lobes represent opposite signs of the wave functions. A relatively large AO represents the major contribution to the MO.

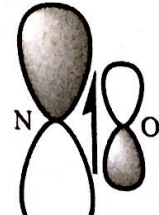
N_2 2σ MO



O_2 $1\pi_g$ MO, doubly degenerate



NO 2π



Dinitrogen with a bond order of three and paired electrons in relatively low energy MOs is very unreactive. Special biological, or industrial, processes are needed to channel energy for promotion of 2π electrons into high-energy, reactive states. The high-energy $1\pi_g$ LUMO is not expected to form stable complexes with electron donors.

Dinitrogen is very stable in most biological organisms, and as a result the task of converting plentiful atmospheric N₂ to the fixed forms of nitrogen that can be incorporated into proteins is a difficult one. The fact that N₂ possesses no unpaired electrons is itself an obstacle to facile reactivity, and the great strength (large dissociation energy) of the N₂ bond is another obstacle. Molecular orbital theory explains both of these obstacles by assigning N₂ a configuration that gives rise to a high bond order (triple bond) with all electrons paired.

Dioxygen is kinetically stable because of a bond order equal to two and a high effective nuclear charge that causes the MOs to have relatively low energy. But two electrons are in the high-energy $1\pi_g$ HOMO level, which is doubly degenerate. These two electrons are unpaired and can contribute to bonding of dioxygen with other species such as the atomic radicals Fe(II) of haemoglobin and Cu(II) of the electron-transport chain. When sufficient, though not excessively large, energy is available, biological processes can channel an electron into this HOMO to produce the reactive superoxide anion of bond order $1\frac{1}{2}$. As a result, O₂ is very reactive in biological systems in ways that promote function (such as respiration) and in ways that disrupt it (damaging cells).

Although the bond order of nitric oxide is $2\frac{1}{2}$, the nitrogen nucleus has a smaller effective nuclear charge than an oxygen atom would have. Thus, the one electron of the 2π HOMO is a high-energy, reactive radical compared to the HOMO of dioxygen. Additionally, the HOMO, being antibonding and predominantly centered on the nitrogen atom, is expected to bond through the nitrogen. Oxidation can result from the loss of the radical electron to form the nitrosyl ion, NO⁺, which has a bond order equal to 3. Even though it has a rather high bond order, NO is readily converted to the damagingly reactive peroxy nitrite ion (ONOO⁻) by reaction with O₂⁻—without breaking the NO linkage.

D10.5

The following list identifies, and justifies, the approximations used in the simple Hückel theory of hydrocarbon π -electron systems.

- Only the carbon p_z valence orbitals of sp²-hybridized carbon atoms contribute to the LCAO of the π system. This is justified to an extent because the hybridization approximation gives reasonable estimates in many instances and p_z orbitals do not overlap with sp²-hybridized orbitals.
- All terms of the form S_{AA} are set equal to 1 and terms of the form S_{AB} are set equal to zero. Overlap integrals between neighbors have small values (even smaller for nonadjacent neighbors) and their neglect eases the mathematics so that an indication of the molecular orbital energy-level diagram can be obtained.
- All terms of the form H_{AA} equal α (a negative quantity). The electronic environment of each sp²-hybridized carbon is very similar, thereby, making all p_z valence orbitals equal in size and energy.
- All terms of the form H_{AB} equal β (a negative quantity) if the atoms are neighbors and to zero otherwise. In addition to a justification similar to that for H_{AA} , when A and B are not neighbors the p_{zA} orbital overlap with the p_{zB} orbital is negligibly small.

These approximations are obviously very severe, but they let us calculate at least a general picture of the molecular orbital energy levels with very little work.

E10.9

The three valence-bond wavefunctions for N_2 are of the form described by eqn 10.1.

$$\psi_1(\sigma\text{-bond}) = \psi_{2p_A}(1) \psi_{2p_B}(2) + \psi_{2p_A}(2) \psi_{2p_B}(1)$$

$$\psi_2(\pi\text{-bond}) = \psi_{2p_A}(1) \psi_{2p_B}(2) + \psi_{2p_A}(2) \psi_{2p_B}(1)$$

$$\psi_3(\pi\text{-bond}) = \psi_{2p_A}(1) \psi_{2p_B}(2) + \psi_{2p_A}(2) \psi_{2p_B}(1)$$
E10.10

The repulsion between two nuclei at $R = 74.1$ pm and $Z = 1$ is given by Coulomb's law.

$$V_{\text{nuc,nuc}} = \frac{e^2}{4\pi\epsilon_0 R} = \frac{(1.602 \times 10^{-19} \text{ C})^2}{(1.113 \times 10^{-10} \text{ J}^{-1} \text{ C}^2 \text{ m}^{-1}) \times (74.1 \times 10^{-12} \text{ m})}$$

$$= 3.11 \times 10^{-18} \text{ J}$$

The molar value is

$$N_A V_{\text{nuc,nuc}} = (6.022 \times 10^{23} \text{ mol}^{-1}) \times (3.11 \times 10^{-18} \text{ J}) = \boxed{1.87 \times 10^6 \text{ J mol}^{-1}}$$

E10.11


There are two localized S—O σ -bonds formed from S(sp^2) and O(p_z) orbitals. There is a π -bond that exhibits resonance and that can be described as the following superposition of wavefunctions:

$$\psi(\pi\text{-bond}) = (\psi_{2p_{sA}} + \psi_{2p_{sB}}) + (\psi_{2p_{zA}} + \psi_{2p_{zB}})$$

The sulfur has a lone pair.



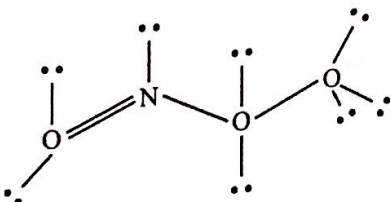
There are three localized S—O σ -bonds from S(sp^2) and O(p_z) orbitals. There is a π -bond that exhibits resonance and that can be described as the following superposition of wavefunctions:

$$\psi(\pi\text{-bond}) = (\psi_{2p_{sA}} + \psi_{2p_{sB}}) + (\psi_{2p_{zA}} + \psi_{2p_{zB}}) + (\psi_{2p_{zC}} + \psi_{2p_{sC}})$$

In the above OA, OB, and OC refer to oxygen atoms A, B, and C.

E10.12

The ion has 24 valence electrons as shown in the Lewis structure. The hybridizations are (from left to right) sp^2 for the first O atom and for the N and sp^3 for the next two O atoms. The first bond is a double bond whose σ component arises from the overlap of sp^2 orbitals and whose π component comes from overlap of unhybridized p orbitals. The next bond is a σ bond involving N sp^2 and O sp^3 orbitals. The O—O bond is a σ bond involving sp^3 orbitals.


E10.13

Refer to the structure shown below in Figure 10.1 for the numbering of the carbon atoms in cis-retinal. Carbon atoms 5–15 each have three sp^2 hybrid atomic orbitals which form σ bonds with

their neighboring atoms. There are six conjugated π bonds between these 11 C atoms and the one O atom. These six π bonds are formed from 12 p_x atomic orbitals, one on each of the 12 atoms. They are resonance hybrids all of the form:

$$\psi(\pi\text{-bond}) = \sum_{i=5}^{15} \psi_{2p_iC_i} + \psi_{2p_iO}$$

All the remaining C atoms each have four sp^3 hybrid atomic orbitals that form σ bonds with their neighboring atoms.

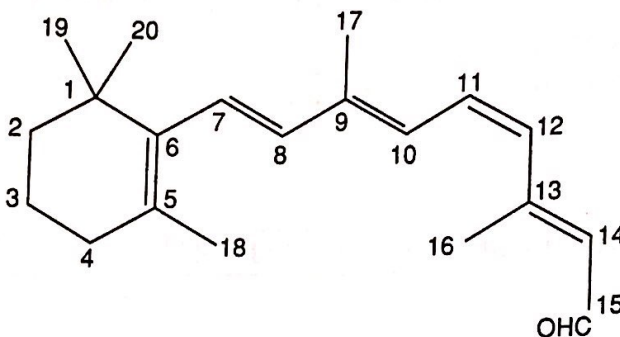


Figure 10.1

E10.14 The atomic orbital ϕ is normalized when $\int \phi^2 d\tau = 1$, where the integral over τ represents an integral over all possible values of x , y , and z . Two atomic orbitals ϕ_1 and ϕ_2 are orthogonal if $\int \phi_1 \phi_2 d\tau = 0$. Each AO of the set s , p_x , p_y , and p_z is both normalized and orthogonal to other members of the set so they are said to be an **orthonormal** set.

$$h_1 = s + p_x + p_y + p_z \quad \text{and} \quad h_2 = s - p_x - p_y + p_z$$

h_1 and h_2 are orthogonal providing that $\int h_1 h_2 d\tau = 0$. We check that this condition is satisfied.

$$\begin{aligned} \int h_1 h_2 d\tau &= \int (s + p_x + p_y + p_z)(s - p_x - p_y + p_z) d\tau \\ &= \int (s^2 - sp_x - sp_y + sp_z) d\tau + \int (sp_x - p_x^2 - p_x p_y + p_x p_z) d\tau \\ &\quad + \int (sp_y - p_x p_y - p_y^2 + p_y p_z) d\tau + \int (sp_z - p_x p_z - p_y p_z + p_z^2) d\tau \end{aligned}$$

All of the above integrals of the type $\int (sp_x) d\tau$ and $\int (p_x p_y) d\tau$ vanish because the integrand AOs are orthogonal. Therefore,

$$\begin{aligned} \int h_1 h_2 d\tau &= \int (s^2) d\tau - \int (p_x^2) d\tau - \int (p_y^2) d\tau + \int (p_z^2) d\tau \\ &= 1 - 1 - 1 + 1 \text{ because the AO are normalized} \\ &= 0 \end{aligned}$$

Thus, h_1 and h_2 are orthogonal.

E10.15 We need to demonstrate that $\int h_{sp^2}^2 d\tau = 1$, where $h_{sp^2} = \frac{s + \sqrt{2}p}{\sqrt{3}}$.

$$\begin{aligned} \int h_{sp^2}^2 d\tau &= \frac{1}{3} \int (s + \sqrt{2}p)^2 d\tau \\ &= \frac{1}{3} \int (s^2 + 2p^2 + 2\sqrt{2}sp) d\tau \\ &= \frac{1}{3}(1 + 2 + 0) \quad \text{as } \int s^2 d\tau = 1, \int p^2 d\tau = 1, \text{ and } \int sp d\tau = 0 \text{ (orthonormality)} \\ &= 1 \end{aligned}$$

Thus, this hybrid orbital is normalized to 1.

E10.16

Rewrite the normalized sp^2 hybrid orbital of part (b) as $h_1 = \frac{s + \sqrt{2}p_x}{\sqrt{3}}$. This hybrid orbital points along the line l_1 on the x -axis as shown in Figure 10.2. There are two additional sp^2 hybrid orbitals, h_2 and h_3 ; they point along the lines l_2 and l_3 . These three orbitals have the same size and shape. They differ only in the direction to which they point. To construct h_2 , we appropriately weigh the s , p_x , and p_y AOs so that the sum points along l_2 while simultaneously being normalized and orthogonal to h_1 . In order to point along l_2 , the weight of p_y must be positive but the weight of p_x must be negative. Furthermore, as shown in Figure 10.2, the weight of p_y must be $3^{1/2}$ times the weight of p_x . Thus,

$$h_2 = as - bp_x + 3^{1/2}bp_y \quad \text{where the weights } a \text{ and } b \text{ are positive numbers}$$

The values of the weights a and b are found with the orthonormal conditions. The orthogonality of h_1 and h_2 provides a useful relation:

$$\begin{aligned} \int h_1 h_2 d\tau &= \int \left(\frac{s + \sqrt{2}p_x}{\sqrt{3}} \right) (as - bp_x + 3^{1/2}bp_y) d\tau \\ &= \frac{a}{3^{1/2}} \int s^2 d\tau - \frac{2^{1/2}b}{3^{1/2}} \int p_x^2 d\tau \quad \text{because terms like } \int sp_x d\tau \text{ equal zero (orthogonality)} \\ &= \frac{a}{3^{1/2}} - \frac{2^{1/2}b}{3^{1/2}} \quad \text{because the orbitals are normalized} \end{aligned}$$

The above expression equals zero when $a = 2^{1/2}b$ so $h_2 = b(2^{1/2}s - p_x + 3^{1/2}p_y)$. Now, we use the normalization condition $\int h_2^2 d\tau = 1$ to determine the value of b .

$$\begin{aligned} \int h_2^2 d\tau &= b^2 \int (2^{1/2}s - p_x + 3^{1/2}p_y)^2 d\tau \\ &= b^2 \{ 2 \int s^2 d\tau + \int p_x^2 d\tau + 3 \int p_y^2 d\tau \} \quad \text{because terms like } \int sp_x d\tau \text{ equal zero (orthogonality)} \\ &= 6b^2 \quad \text{because the orbitals are normalized} \end{aligned}$$

Thus, $b = 6^{-1/2}$ and substitution gives

$$h_2 = \sqrt{\frac{1}{3}}s - \sqrt{\frac{1}{6}}p_x + \sqrt{\frac{1}{2}}p_y$$

The sp^2 hybrid h_3 is a reflection of h_2 through the y -axis so we need only change the weight of p_y by changing the weight sign, thereby, giving the last of the three sp^2 hybrids.

$$h_3 = \sqrt{\frac{1}{3}}s - \sqrt{\frac{1}{6}}p_x - \sqrt{\frac{1}{2}}p_y$$

Note that our solution here goes somewhat beyond the form of the hybrids listed in eqns 10.2b of the text in that the orbitals here have been normalized and include the normalization factor $\sqrt{\frac{1}{3}}$. Also we arbitrarily switched the x and y labels on orbitals. This is inconsequential.

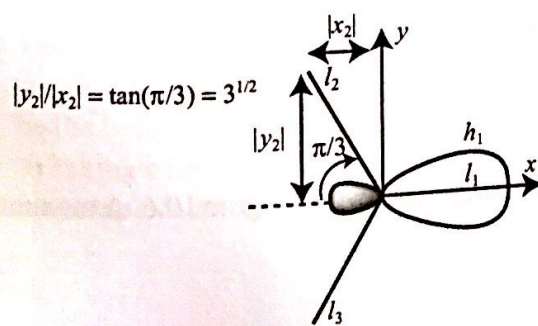


Figure 10.2

E10.17

Covalent structures are shown in Figure 10.3(a), while ionic structures are shown in Figure 10.3(b).

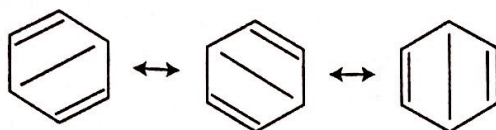


Figure 10.3(a)

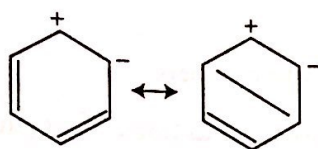


Figure 10.3(b)

In addition, there are many other possible ionic structures. These structures can be safely ignored in simple descriptions of the molecule because the coefficients of the wavefunction representing these structures in the linear combination of wavefunctions for the entire resonance hybrid are very small. Benzene is a very symmetrical molecule, and we expect that all the C atoms will be equivalent. Hence, those structures in which the C atoms are not equivalent should contribute little to the resonance hybrid.

E10.18

When the s orbital shares a common center with the p orbital, the constructive interference between the s orbital and one of the p orbital lobes is exactly balanced with the destructive interference between the s orbital and the other p orbital lobe (see Figure 10.4). Thus, when $R = 0$, $S = 0$. As the two orbitals separate the overlap increases to a maximum after which larger separation results in an ever decreasing overlap, which is sketched in Figure 10.5.

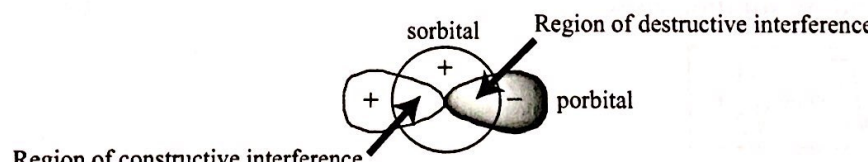


Figure 10.4

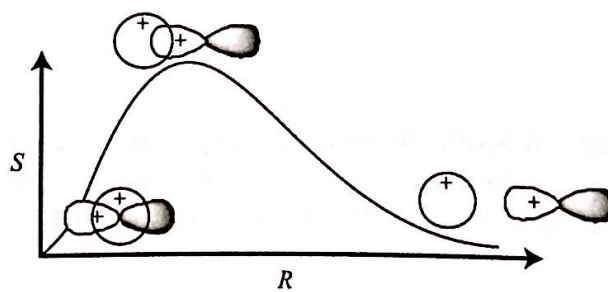


Figure 10.5

$$S = (R/a_0) \{1 + (R/a_0) + \frac{1}{3}(R/a_0)^2\} e^{-R/a_0}$$

Draw up the following table and plot S against R/a_0 as shown in Figure 10.6. A maximum occurs at $R/a_0 = 2.11$.

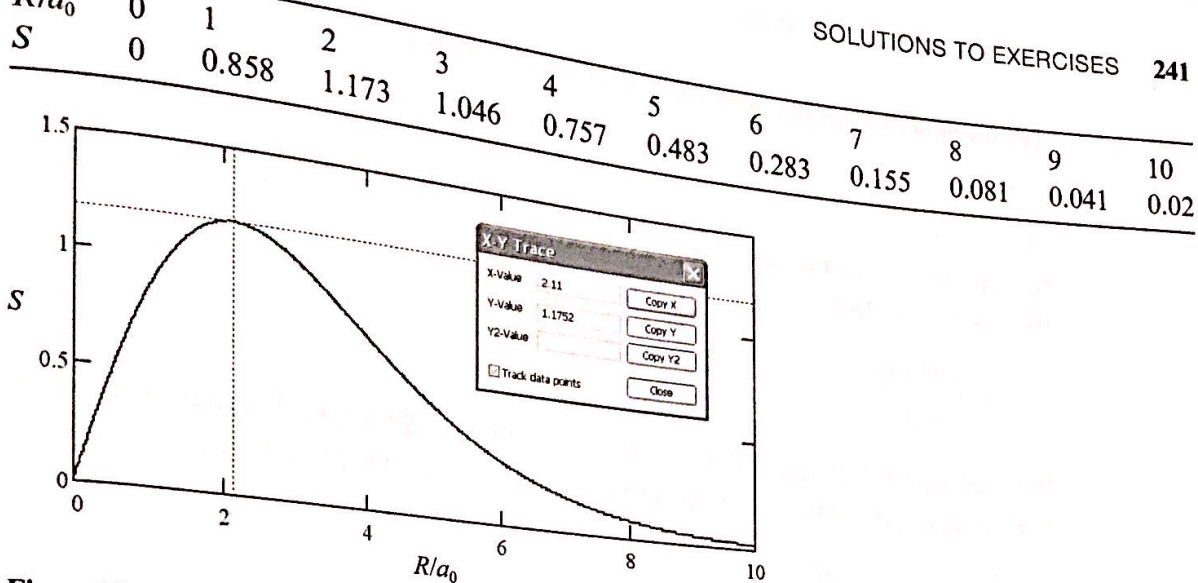


Figure 10.6

E10.19

We seek an orbital of the form $aA + bB$, where a and b are constants, which is orthogonal to the orbital $N(0.245A + 0.644B)$. Orthogonality implies

$$\int(aA + bB)N(0.245A + 0.644B)d\tau = 0$$

$$N \int [0.245aA^2 + (0.245b + 0.644a)AB + 0.644bB^2]d\tau = 0$$

The integrals of squares of orbitals are 1 and the integral $\int ABd\tau$ is the overlap integral S , so

$$0 = (0.245 + 0.644S)a + (0.245S + 0.644)b \quad \text{so} \quad a = -\frac{0.245S + 0.644}{0.245 + 0.644S}b$$

This would make the orbitals orthogonal, but not necessarily normalized. If $S = 0$, the expression simplifies to

$$a = -\frac{0.644}{0.245}b$$

and the new orbital would be normalized if $a = 0.644N$ and $b = -0.245N$. That is

$$N(0.644A - 0.245B)$$

E10.20

In general, we have $\psi = c_A \psi_A + c_B \psi_B$

We need to determine the coefficients c_A and c_B .

A systematic way of finding the coefficients in the linear combinations used to build molecular orbitals is provided by the variation principle:

If an arbitrary wavefunction is used to calculate the energy, then the value calculated is never less than the true energy.

The arbitrary wavefunction is called the trial wavefunction. The principle implies that if we vary the coefficients in the trial wavefunction until we achieve the lowest energy, then those coefficients will be the best. We might get a lower energy if we use a more complicated wavefunction (for example, by taking a linear combination of several atomic orbitals on each atom), but we shall have the optimum molecular orbital that can be built from the given set of atomic orbitals.

The method can be illustrated by the trial wavefunction

$$\psi = c_A \psi_A + c_B \psi_B$$

This function is real but not normalized (because the coefficients can take arbitrary values), so in the following we cannot assume that $\int \psi^2 d\tau = 1$. The energy of the orbital is the expectation value of the energy operator

$$E = \frac{\int \psi H \psi d\tau}{\int \psi^2 d\tau}$$

We must search for values of the coefficients in the trial function that minimize the value of E . This is a standard problem in calculus, and is solved by finding the coefficients for which

$$\frac{\partial E}{\partial c_A} = 0 \quad \text{and} \quad \frac{\partial E}{\partial c_B} = 0$$

The first step is to express the two integrals in terms of the coefficients. The denominator is

$$\begin{aligned} \int \psi^2 d\tau &= \int \{c_A \psi(A) + c_B \psi(B)\}^2 d\tau \\ &= c_A^2 \int \psi(A)^2 d\tau + c_B^2 \int \psi(B)^2 d\tau + 2c_A c_B \int \psi(A) \psi(B) d\tau \\ &= c_A^2 + c_B^2 + 2c_A c_B S \quad (1) \end{aligned}$$

because the individual atomic orbitals are normalized and the third integral is the overlap integral S . The numerator is

$$\begin{aligned} \int \psi H \psi d\tau &= \int \{c_A \psi_A + c_B \psi_B\} H \{c_A \psi_A + c_B \psi_B\} d\tau \\ &= c_A^2 \int \psi_A H \psi_A d\tau + c_B^2 \int \psi_B H \psi_B d\tau + 2c_A c_B \int \psi_A H \psi_B d\tau \end{aligned}$$

There are some complicated integrals in this expression, but we can denote them by the constants

$$\alpha_A = \int \psi(A) H \psi(A) d\tau \quad \alpha_B = \int \psi(B) H \psi(B) d\tau \quad \beta = \int \psi(A) H \psi(B) d\tau$$

Then

$$\int \psi H \psi d\tau = c_A^2 \alpha_A + c_B^2 \alpha_B + 2c_A c_B \beta$$

α is called a **Coulomb integral**. It is negative, and can be interpreted as the energy of the electron when it occupies ψ_A (for α_A) or ψ_B (for α_B). In a homonuclear diatomic molecule, $\alpha_A = \alpha_B$. β is called a **resonance integral** (for classical reasons). It vanishes when the orbitals do not overlap, and at equilibrium bond lengths it is normally negative.

The complete expression for E is

$$E = \frac{c_A^2 \alpha_A + c_B^2 \alpha_B + 2c_A c_B \beta}{c_A^2 + c_B^2 + 2c_A c_B S}$$

Its minimum is found by differentiation with respect to the two coefficients. This involves elementary but slightly tedious work, the end result being the two **secular equations**

$$(\alpha_A - E)c_A + (\beta - ES)c_B = 0$$

$$(\beta - ES)c_A + (\alpha_B - E)c_B = 0$$

They have a solution if the determinant of the coefficients, the *secular determinant* vanishes; that is, if

$$\begin{vmatrix} \alpha_A - E & \beta - ES \\ \beta - ES & \alpha_B - E \end{vmatrix} = 0$$

This determinant expands to a quadratic equation in E , which may be solved. Its two roots give the energies of the bonding and antibonding MOs formed from the basis set and, according to the variation principle, these are the best energies for the given basis set. The corresponding values of the coefficients are then obtained by solving the secular equations using the two energies: the lower energy gives the coefficients for the bonding MO, the upper energy the coefficients for the antibonding MO. The secular equations give expressions for the ratio of the coefficients in each case, and so we need a further equation in order to find their individual values. This is obtained by demanding that the best wavefunction should be normalized, which means that we must also ensure (from eqn (1) above) that

$$\int \psi^2 d\tau = c_A^2 + c_B^2 + 2c_A c_B S = 1.$$

There are two cases where the roots can be written down very simply. First, when the two atoms are the same, and we can write $\alpha_A = \alpha_B = \alpha$, the solutions are

$$E_+ = \frac{\alpha + \beta}{1 + S} \quad c_A = \left\{ \frac{1}{2(1 + S)} \right\}^{1/2} \quad c_B = c_A$$

$$E_- = \frac{\alpha - \beta}{1 - S} \quad c_A = \left\{ \frac{1}{2(1 - S)} \right\}^{1/2} \quad c_B = -c_A$$

In this case, the best bonding function has the form

$$\psi_+ = \left\{ \frac{1}{2(1 + S)} \right\}^{1/2} \{ \psi_A + \psi_B \}$$

and the corresponding antibonding function is

$$\psi_- = \left\{ \frac{1}{2(1 - S)} \right\}^{1/2} \{ \psi_A - \psi_B \}$$

(a) When it is justifiable to neglect overlap, the secular determinant is

$$\begin{vmatrix} \alpha_A - E & \beta \\ \beta & \alpha_B - E \end{vmatrix} = 0$$

and its solutions can be expressed in terms of the parameter θ , with

$$\tan(2\theta) = \frac{2\beta}{\alpha_A - \alpha_B}$$

The solutions are:

$$E_- = \alpha_A - \beta \cot \theta \quad \psi_- = -\sin \theta \psi_A + \cos \theta \psi_B$$

$$E_+ = \alpha_B + \beta \cot \theta \quad \psi_+ = \cos \theta \psi_A + \sin \theta \psi_B$$

If $\theta = 0$, the wavefunction $\psi_+ = \psi_A$; if $\theta = \pi/2$, the wavefunction $\psi_+ = \psi_B$. So we see that this wavefunction can describe a polar covalent bond, the degree of polarity is dependent on θ . If $\theta = \pi/4$, the bond is completely covalent.

(b) We need to evaluate $\int \psi^2 d\tau$ to see if it equals 1.

$$\begin{aligned} \int (\psi_A \cos \theta + \psi_B \sin \theta)^2 d\tau &= \int (\psi_A^2 \cos^2 \theta + \psi_B^2 \sin^2 \theta + 2\psi_A \psi_B \sin \theta \cos \theta) d\tau \\ &= \cos^2 \theta \int \psi_A^2 d\tau + \sin^2 \theta \int \psi_B^2 d\tau + 2 \sin \theta \cos \theta \int \psi_A \psi_B d\tau \\ &= \cos^2 \theta + \sin^2 \theta + 2 \sin \theta \cos \theta S \end{aligned}$$

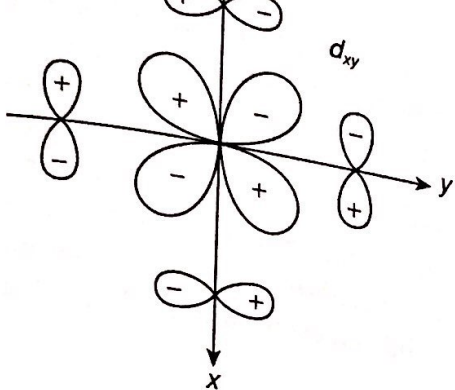


Figure 10.9

E10.22

The total number of atomic orbitals in a single set of s, p, d, and f subshells is
 $1 + 3 + 5 + 7 = 16$

In a diatomic molecule there would then be 32 AO from which 32 molecular orbitals can be

E10.23

- | | | |
|--------------------|---|-------------------|
| (a) H ₂ | $1\sigma_g^2 1\sigma_u^1$ | |
| (b) N ₂ | $1\sigma_g^2 1\sigma_u^1 1\pi_u^4 2\sigma_g^2$ | $b = \frac{1}{2}$ |
| (c) O ₂ | $1\sigma_g^2 1\sigma_u^2 2\sigma_g^2 1\pi_u^4 1\pi_g^2$ | $b = 3$ |
| | | $b = 2$ |

E10.24

- | | | |
|---------------------|---|-------------------|
| (a) CO | $1\sigma^2 2\sigma^* 2 1\pi^4 3\sigma^2$ | $b = 3$ |
| (b) NO | $1\sigma^2 2\sigma^* 2 1\pi^4 3\sigma^2 2\pi^*$ | $b = \frac{5}{2}$ |
| (c) CN ⁻ | $1\sigma^2 2\sigma^* 2 1\pi^4 3\sigma^2$ | $b = 3$ |

E10.25

Decide whether the electron added or removed increases or decreases the bond order. The simplest procedure is to decide whether the electron occupies or is removed from a bonding or antibonding orbital. The levels for the homonuclear diatomics are shown in text Figures 10.30 and 10.31. The level for the heteronuclear diatomics is shown in text Figure 10.35.

The following table gives the orbital involved

	N ₂	NO	O ₂	C ₂	F ₂	CN
(a) AB ⁻	$1\pi_g$	2π	$1\pi_g$	$2\sigma_g$	$2\sigma_u$	3σ
Δb	$-\frac{1}{2}$	$-\frac{1}{2}$	$-\frac{1}{2}$	$+\frac{1}{2}$	$-\frac{1}{2}$	$+\frac{1}{2}$
(b) AB ⁺	$2\sigma_g$	2π	$1\pi_g$	$1\pi_u$	$1\pi_g$	3σ
Δb	$-\frac{1}{2}$	$+\frac{1}{2}$	$+\frac{1}{2}$	$-\frac{1}{2}$	$+\frac{1}{2}$	$-\frac{1}{2}$

Therefore,

C₂ and CN are stabilized by anion formation. NO, O₂, and F₂ are stabilized by cation formation

E10.26

The wavefunctions are

$$\psi_n(x) = \left(\frac{2}{L}\right)^{1/2} \sin\left(\frac{n\pi x}{L}\right) \text{ [Chapter 9], where } n=1,2,3,\dots \text{ and } 0 < x < L$$

Each of these wavefunctions has a center of symmetry at L/2 so we invert through x = $\frac{L}{2}$. For n = 1, when $x < \frac{L}{2}$, $\psi_1 = +$, when $x > \frac{L}{2}$, $\psi_1 = -$, therefore ψ_1 is \boxed{g} . In a similar fashion we determine

$$n = 2, \boxed{u}; n = 3, \boxed{g}; n = 4, \boxed{u}.$$

Figure 10.10 below illustrates the operation of inversion through the center of symmetry. First, identify the center of symmetry. Then, pick any non-nodal position and note the sign and magnitude of the wavefunction. Draw an arrow from that wavefunction point through the center of symmetry to a point that is an equal distance on the opposite side of the center of symmetry. If the wavefunction has the same magnitude and sign after the inversion, the wavefunction has gerade (g) symmetry. If the wavefunction has the same magnitude and opposite sign, the wavefunction has ungerade (u) symmetry. We quickly see that all odd-numbered ($n = 1, 3, 5, \dots$) quantum states of the particle in a box have gerade symmetry or "parity" while all even-numbered ($n = 2, 4, 6, \dots$) states have ungerade symmetry or "parity".

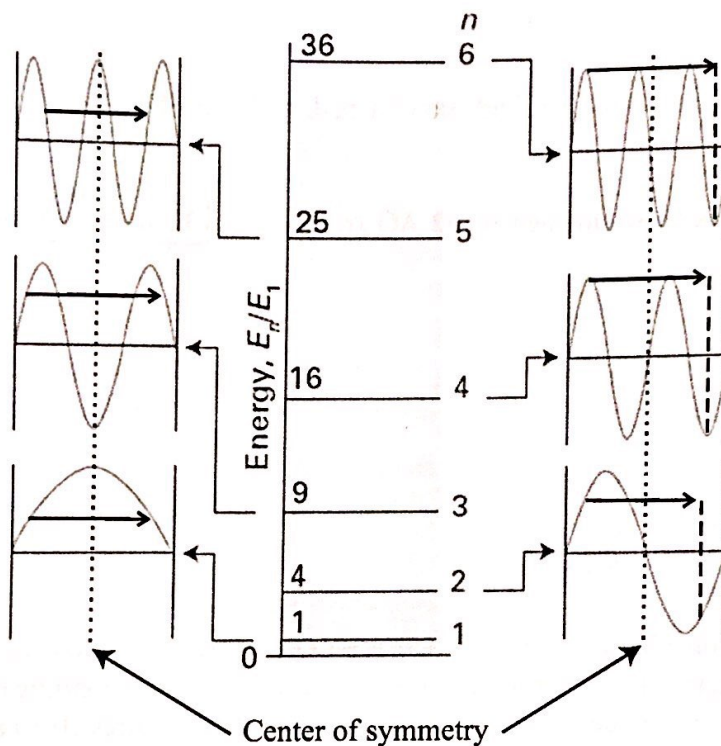


Figure 10.10

- E10.27** Refer to Figure 9.39(a) of the text. Examine the inversion through the center of these functions, i.e. replace x with $-x$.

(a) $\nu = 0, \boxed{g}$

$\nu = 1, \boxed{u}$

$\nu = 2, \boxed{g}$

$\nu = 3, u$ (Figure 9.39(a) of the text)

- (b) If ν is even, ψ_ν is g.

If ν is odd, ψ_ν is u.

- E10.28** The parities can be deduced from Figure 10.39 of the text:

Orbital at $\alpha + 2\beta$ has u parity.

Doubly degenerate orbitals at $\alpha + \beta$ have g parity.

Doubly degenerate orbitals at $\alpha - \beta$ have u parity.

Orbital at $\alpha - 2\beta$ has g parity.

Molecules and self-assembly

Answers to discussion questions

D11.1

The X-ray diffraction pattern of fibrous B-DNA, shown in both text Figure 11.6 and Figure 11.1 below, provides a seminal example of a diffraction pattern of a helical conformation of a macro-molecule. Features are discussed in Case Study 11.1. *The structure of DNA from X-ray diffraction studies.* This particular pattern was obtained with a fiber consisting of many DNA molecules oriented with their axes parallel to the axis of the fiber, with X-rays incident from a perpendicular direction. All the molecules in the fiber are parallel (or nearly so) but are randomly distributed in the perpendicular directions; as a result, the diffraction pattern exhibits the periodic structure parallel to the fiber axis superimposed on a general background of scattering from the distribution of molecules in the perpendicular directions.

Each turn of a helix defines two planes, shown in text Figure 11.22, one orientated at an angle α to the horizontal and the other at $-\alpha$. As a result, to a first approximation, a helix can be thought of as consisting of an array of planes at an angle α to the horizontal together with an array of planes at an angle $-\alpha$ with a separation within each set determined by the pitch p , which is the vertical rise per turn of the helix. Thus, a DNA molecule is like two arrays of planes, each set corresponding to those treated in the derivation of the Bragg law, with a perpendicular separation $d = p \cos \alpha$. The diffraction spots from one set of planes therefore occur at an angle α to the vertical, giving one leg of the X character of the diffraction pattern, and those of the other set occur at an angle $-\alpha$, giving rise to the other leg of the pattern. The experimental arrangement has up-down symmetry, so the diffraction pattern repeats to produce the lower half of the X. The sequence of spots outward along a leg corresponds to first-, second-,... order diffraction ($n = 1, 2, \dots$ in eqn 11.11b). Figure 11.2 serves to illustrate the reflections off the two sets of planes that form the angle 2α ; it also shows the definitions of d and p .

As an aid to understanding the B-DNA X-ray diffraction pattern we represent the nucleotide bases by points as shown in text Figure 11.23 and see that there is an additional periodicity of separation h , forming planes that are perpendicular to the axis to the molecule (and the fiber). These planes give rise to the strong meridional diffraction at the top and bottom of the pattern with an angle that allows us to determine the layer spacing from Bragg's law.

The characteristic X-shape of the B-DNA diffraction pattern shown in Figure 11.1 is that of a helix with incident radiation (Cu K_α 0.1542 nm) perpendicular to the cylindrical axis. An angle $\theta = 2.6^\circ$ between the line of the incident radiation and the line from the sample to the first spot on the X gives $p = \lambda/\sin \theta = 0.1542 \text{ nm}/\sin(2.6^\circ) = 3.4 \text{ nm}$. 10 spots (counting two "missing fourth" spots) along the X diagonal indicate that there are 10 base-planes per turn of the helix with each accounting for a turn of 40° . The very large spot is at a distance ($1/h$) that is 10 times the distance $1/p$ shown in the diagram. Consequently, $h = 0.34 \text{ nm}$. The missing fourth spots on the X diagonals indicate two coaxial sugar-phosphate backbones that are separated by $3p/8$ along the axis. The periodic h spacing of the large, very electron-dense phosphorous atoms in the sugar-phosphate backbone of

the macromolecule causes the $1/h$ spots to be very intense. The fact that the fibrous X-ray sample was saturated with water suggests that the phosphates are to the outside.

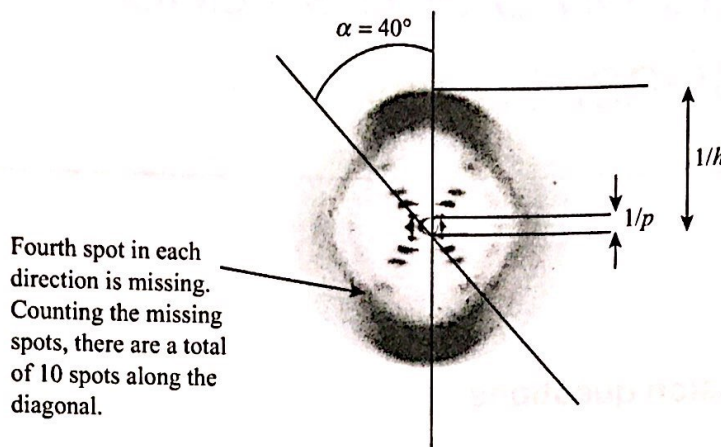


Figure 11.1

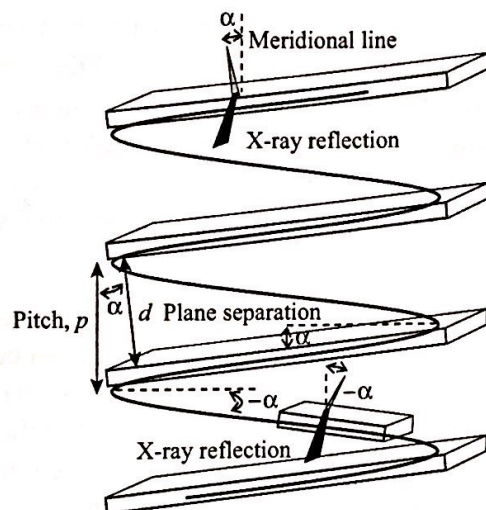


Figure 11.2

Figure 11.3 shows the two-dimensional zig-zag projection of the helical sugar-phosphate backbone onto a plane along the central axis. It serves to show the definitions of the projection length l , perpendicular distance d between backbone planes, and the helix radius r . Examination of the right triangle that shows the definition of α yields:

$$\tan(\alpha) = \frac{p}{4r} \quad \text{or} \quad r = \frac{p}{4 \tan(\alpha)} = \frac{3.4 \text{ nm}}{4 \tan(40^\circ)} = 1.0 \text{ nm}$$

Examination of the right triangle containing the angle α also shows that $l \sin(\alpha) = p/2$, while the right triangle containing the angle 2α shows that $l \sin(2\alpha) = d$. Dividing these two equations yields:

$$\frac{\sin(2\alpha)}{\sin(\alpha)} = \frac{2d}{p} \quad \text{or} \quad \frac{2 \sin(\alpha) \cos(\alpha)}{\sin(\alpha)} = \frac{2d}{p} \quad \text{or} \quad \cos(\alpha) = \frac{d}{p}$$

$$d = p \cos(\alpha) = (3.4 \text{ nm}) \cos(40^\circ) = 2.6\bar{0} \text{ nm}$$

Finishing,

$$l = \frac{p}{2 \sin(\alpha)} = \frac{3.4 \text{ nm}}{2 \sin(40^\circ)} = 2.6\bar{5} \text{ nm}$$

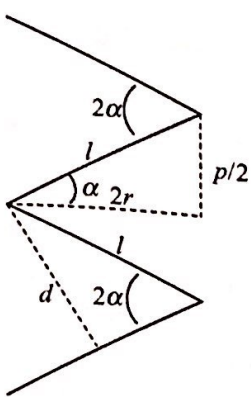


Figure 11.3

D11.2

The structure factor F_{hkl} is the sum over all j atoms of terms each of which has a scattering factor f_j :

$$F_{hkl} = \sum_j f_j e^{i\phi_{hkl}(j)}, \quad \text{where } \phi_{hkl}(j) = 2\pi(hx_j + ky_j + lz_j)$$

The importance of the structure factor to the X-ray crystallographic method of structure determination is its **Fourier synthesis** relationship to the electron density distribution, $\rho(r)$, within the crystal:

$$\rho(r) = \frac{1}{V} \sum_{hkl} F_{hkl} e^{-2\pi i(hx+ky+lz)} \quad [\text{generalization of eqn 11.12}].$$

The Fourier synthesis reveals that, if the structure factors for the lattice planes can be measured, the electron density distribution can be calculated by performing the indicated sum. Therein lies the **phase problem**. Measurement detectors yield only the intensity of scattered radiation, which is proportional to $|F_{hkl}|^2$, and give no direct information about F_{hkl} . To see this, consider the structure factor form $F_{hkl} = |F_{hkl}| e^{i\alpha_{hkl}}$, where α_{hkl} is the phase of the hkl reflection plane. Then,

$$|F_{hkl}|^2 = \{|F_{hkl}| e^{i\alpha_{hkl}}\} * \{|F_{hkl}| e^{i\alpha_{hkl}}\} = |F_{hkl}| \times |F_{hkl}| e^{-i\alpha_{hkl}} e^{i\alpha_{hkl}} = |F_{hkl}| \times |F_{hkl}|$$

and we see that all information about the phase is lost in an intensity measurement. It seems impossible to perform the sum of the Fourier synthesis since we do not have the important factor $e^{i\alpha_{hkl}}$. Crystallographers have developed numerous methods to resolve the phase problem. In the **Patterson synthesis**, X-ray diffraction spot intensities are used to acquire separation and relative orientations of atom pairs. Another method uses the dominance of heavy-atom scattering to deduce phase. **Heavy-atom replacement** may be necessary for this type of application. **Direct methods** dominate modern X-ray diffraction analysis. These methods use statistical techniques, and the considerable computational capacity of the modern computer, to compute the probabilities that the phases have a particular value.

D11.3

Molecules with a permanent separation of electric charge have a **permanent dipole moment** μ . In molecules containing atoms of differing electronegativity, the bonding electrons may be displaced in such a way as to produce a net separation of charge in the molecule. Separation of charge may also arise from a difference in the atomic radii of the bonded atoms. The separation of charges in the bonds is usually, though not always, in the direction of the more electronegative atom but depends on the precise bonding situation in the molecule as described in Section 11.6. A heteronuclear diatomic molecule necessarily has a dipole moment if there is a difference in electronegativity between the atoms, but the situation in polyatomic molecules is more complex. A polyatomic molecule has a permanent dipole moment only if at least one of its μ_x , μ_y , μ_z components is non-zero (see eqn 11.15a). Thus, the tetrahedral CCl_4 molecule has polar bonds but the sums of the polar components balance so as to cancel and give $\mu = 0$. Molecular symmetry is reduced in $CHCl_3$, a molecule that has a permanent dipole moment because the C-H bond does not balance the polarity

of the C–Cl bonds. Similarly, 1,4-dichlorobenzene is non-polar, while 1,2-dichlorobenzene is a polar molecule.

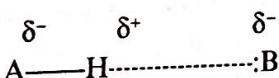
QUESTION: Why does a molecule of trans-1,4-dichlorocyclohexane have no permanent dipole while a molecule of cis-1,4-dichlorocyclohexane does have a permanent dipole?

See the discussion of ozone and carbon dioxide in Section 11.6 for further examples of the importance of molecular symmetry and electronegativities in deciding whether a polyatomic molecule is polar or not. The discussion of carbon monoxide is a very important example of a molecule that has a dipole moment in the opposite direction to that expected from electronegativity considerations alone because the polarity of the HOMO antibonding orbital, which is reversed from the electronegativity expectation, provides a large contribution to the observed polarity.

Both non-polar and polar molecules may acquire a temporary induced dipole moment μ^* as a result of the influence of an electric field E generated by a nearby ion or polar molecule. The field distorts the electron distribution of the molecule, and gives rise to an electric dipole. The induced dipole moment is proportional to the field [11.19] and the constant of proportionality is called the polarizability α . Molecular structure features that affect polarizability include molecular size, nuclear control, ionization energy, and the relative orientation of the molecule with the external electric field.

D11.4 A hydrogen bond (...) is an attractive interaction between two species that arises from a link of the form A–H \cdots B, where A and B are highly electronegative elements (usually nitrogen, oxygen, or fluorine) and B possesses a lone pair of electrons. It is a contact-like attraction that requires AH to touch B. Experimental evidence supports a linear or near-linear structural arrangement and a bond strength of about 20 kJ mol $^{-1}$. The hydrogen bond strength is considerably weaker than a covalent bond but it is larger than, and dominates, other intermolecular attractions such as dipole–dipole attractions. Its formation can be understood in terms of either the (a) electrostatic interaction model or with (b) molecular orbital calculations.

(a) A and B, being highly electronegative, are viewed as having partial negative charges (δ^-) in the electrostatic interaction model of the hydrogen bond. Hydrogen, being less electronegative than A, is viewed as having a partial positive (δ^+). The linear structure maximizes the electrostatic attraction between H and B:



This model is conceptually very useful. However, it is impossible to exactly calculate the interaction strength with this model because the partial atomic charges cannot be precisely defined. There is no way to define which fraction of the electrons of the AB covalent bond should be assigned to one or the other nucleus.

(b) *Ab initio* MO quantum calculations are needed in order to explore questions about the linear structure, the role of the lone pair, the shape of the potential energy surface, and the extent to which the hydrogen bond has covalent sigma bond character. Yes, the hydrogen bond appears to have some sigma bond character. This was initially suggested by Linus Pauling in the 1930s and more recent experiments with Compton scattering of X-rays and NMR techniques indicate that the covalent character may provide as much as 20% of the hydrogen bond strength. A three-center molecular orbital model provides a degree of insight. A linear combination of an appropriate sigma orbital on A, the 1s hydrogen orbital, and an appropriate orbital for the lone pair on B yields a total of three molecular orbitals of the form:

$$\psi = c_1\psi_A + c_2\psi_H + c_3\psi_B$$

One of the MOs is bonding, one is almost non-bonding, and the third is antibonding (see text Figure 11.29). Both the bonding MO and the almost non-bonding orbital are occupied by two

electrons (the sigma bonding electrons of A–H and the lone pair of B). The antibonding MO is empty. Thus, depending on the precise location of the almost non-bonding orbital, the non-bonding orbital may lower the total energy and account for the hydrogen bond.

D11.5

Contour length, R_c : the length of the macromolecule measured along its backbone, the length of all its monomer units placed end to end. This is the stretched-out length of the macromolecule with bond angles maintained within the monomer units and 180° angles at unit links. It is proportional to the number of monomer units, N , and to the length of each unit [11.29].

Root mean square separation, R_{rms} : one measure of the average separation of the ends of a random coil. It is the square root of the mean value of R^2 , where R is the separation of the two ends of the coil. R_{rms} is proportional to $N^{1/2}$ and the length of each unit [11.28].

Radius of gyration, R_g : the radius of a thin hollow spherical shell of the same mass and moment of inertia as the macromolecule. In general, it is not easy to visualize this distance geometrically. However, for the simple case of a molecule consisting of a chain of identical atoms this quantity can be visualized as the root mean square distance of the atoms from the center of mass. It also depends on $N^{1/2}$, but is smaller than the root mean square separation by a factor of $(1/6)^{1/2}$ [11.30].

D11.6

$$(a) V = -\frac{Q_2 \mu_1}{4\pi\epsilon_0 r^2} \quad [11.16a]$$

V is the potential energy of interaction between a point dipole μ_1 and the point charge Q_2 at the separation r . The point charge lies on the axis of the dipole and the separation r is much larger than the separation of charge within the dipole so that the partial charges of the dipole seem to merge and cancel to create the so-called **point dipole**.

$$(b) V = -\frac{Q_2 \mu_1 \cos\theta}{4\pi\epsilon_0 r^2} \quad [11.16b]$$

V is the potential energy of interaction between a point dipole μ_1 and the point charge Q_2 at the separation r . The point charge lies at an angle θ to the axis of the dipole and the separation r is much larger than the separation of charge within the dipole so that the partial charges of the dipole seem larger than the separation of charge within the dipole so that the partial charges of the dipole seem to merge and cancel.

$$(c) V = \frac{\mu_1 \mu_2 f(\theta)}{4\pi\epsilon_0 r^3}, \quad \text{where } f(\theta) = 1 - 3 \cos^2 \theta \quad [11.17]$$

V is the potential energy of interaction between the two point dipoles μ_1 and μ_2 at the separation r . The dipoles are parallel and the separation distance is at angle θ to the dipoles. The separation r is much larger than the separation of charge within the dipoles so that the partial charges of the dipoles seem to merge and cancel.

$$(d) R_{rms} = N^{1/2} l$$

Each of N monomers occupies length l along the polymer chain. R_{rms} is the root mean square separation between the ends of the polymer chain when the polymer is modeled as a freely jointed chain in which any bond between two monomer residues is free to make any angle with respect to the previous one. This random-coil model ignores the volume occupied by each residue, electronic restrictions on bond angles, and solvent effects.

$$(e) R_g = (N/6)^{1/2} l$$

Each of N monomers occupies length l along the polymer chain, which is modeled as a freely jointed chain. R_g is the radius of gyration of the randomly coiled polymer. That is, R_g is the radius of a thin shell that has the same mass and the same moment of inertia as the coiled polymer.